Discover Materials

Discover

Research

A molecular route to fluoro-perovskite materials: synthesis of $CsCaF_3$ films through a sol–gel/spin-coating process

Anna L. Pellegrino[1] · Francesca Lo Presti[1] · Graziella Malandrino[1]

Received: 4 February 2022 / Accepted: 9 May 2022
Published online: 21 May 2022

Abstract
Fluoride perovskites have recently attracted great attention due to their unique optical properties. The present study reports for the first time the fabrication of fluoride-based perovskite, $CsCaF_3$, in form of thin films through a combined sol–gel/spin-coating approach using β-diketonate fluorinated precursors. The entire sol–gel process has been carried out in ethanol solution under acid-catalyzed conditions starting from the β-diketonate complexes, Cs(hfa) and $Ca(hfa)_2$•diglyme•H_2O (Hhfa = 1,1,1,5,5,5-hexafluoro-2,4-pentanedione; diglyme = 2–Methoxyethylether), which act as single sources for metal ions and fluorine**.** A careful optimization of the process parameters, such as molar ratio of the starting mixture, aging time and annealing temperature, has allowed to produce for the first time, selectively and reproducibly, transparent and pure $CsCaF_3$ films. Field-emission scanning electron microscopy and energy dispersive X-ray analyses highlight the formation of films with compact morphologies having a 1:1 stoichiometric ratio of Cs:Ca, uniform throughout the film and compatible with the $CsCaF_3$ phase identified through X-ray diffraction analysis.

Keywords Fluoride perovskite · Thin films · Single-precursor · Sol–gel

1 Introduction

Halide perovskites are nowadays key materials for many technologies in several application fields ranging from photovoltaics [1, 2], to piezoelectrics and multiferroics [3, 4] from catalysis [5] to optics [6].

Recently, there has been an increasing interest on the research of new, stable and industrially appealing fluoride-based perovskite materials. In particular, $MCaF_3$ structures, with M = K, Rb and Cs, have been the subject of study for their optoelectronic properties useful for transparent optical coatings [7], fast scintillators [8] and phosphors for radiation dosimetry when doped with lanthanide ions [9]. Among them, $CsCaF_3$ represents one of the most interesting materials due to its stability and electronic properties. In this context, several theoretical studies have been conducted in order to deeply explore most of the relevant parameters, such as electronic band gaps and hole effective masses [10–13].

There are various key issues to be addressed for the wide application of this class of compounds, such as the presence of abundant and non-toxic elements and the thermodynamic stability, which gives additional advantages in terms of easy production and resistance to radiation or heat.

Supplementary Information The online version contains supplementary material available at https://doi.org/10.1007/s43939-022-00025-3.

✉ Anna L. Pellegrino, annalucia.pellegrino@unict.it; ✉ Graziella Malandrino, graziella.malandrino@unict.it | [1]Dipartimento di Scienze Chimiche, Università Degli Studi di Catania, INSTM UdR Catania, Viale Andrea Doria 6, 95125 Catania, Italy.

Recently, Körbel et al. [14], using a density functional theory-based approach, reported a comprehensive study on nearly 200 possible and stable ABX_3 perovskites as ideal cubic or slightly distorted structure with X non-metal and A and B various metals of the periodic table. Most of them have been identified as new structures missing in the databases. It has been demonstrated that such compounds are thermodynamically stable by calculating various electronic properties, i.e. electronic band gap, hole effective mass, and spontaneous ferroelectric and magnetic polarization [14]. Among them, $CsCaF_3$ is one of the stable structures with a band gap calculation ranging from 6.9 to 9.8 eV, depending on the theoretical applied methodology [11, 15]. Additionally, a change of the band gap character from indirect to direct, going from K to Cs in $MCaF_3$ (M = K, Rb and Cs) structures has been observed in most of the calculations [16].

Despite the theoretical research efforts, the number of papers on experimental approaches to synthesize the $CsCaF_3$ phase is exiguous. To the best of our knowledge, only few papers report the synthesis of $CsCaF_3$, and none of them report the fabrication in form of thin film. The synthetic strategy is based on the formation of $CsCaF_3$ microcrystals starting from calcium and cesium fluorides at high temperature and pressure [17]. Recently, Falin et al. [18] have reported the fabrication, through a Bridgman—Stockbarger method, of $CsCaF_3$ crystals and have studied the effect of the Yb^{3+} ion doping on the structure and on the paramagnetic and luminescence properties.

Therefore, in order to explore the wide potentiality of the $CsCaF_3$ system, the development of new synthetic strategies to deposit thin films remains an open issue.

Recently, our group developed a pioneering process for the synthesis of ternary fluoride phase, such as $NaYF_4$, testing different sol–gel routes starting from the fluorinated β-diketonate adducts Na(hfa)•tetraglyme and $Y(hfa)_3$•diglyme [19, 20]. The optimization of the process involved various molar ratios, aging time of the sol and spin coating deposition process.

Herein, an innovative method for the synthesis of $CsCaF_3$ system in form of thin films is reported for the first time through a combined sol–gel and spin-coating approach. The starting point has been the use of β-diketonate fluorinated precursors of Cs and Ca, i.e. Cs(hfa) and $Ca(hfa)_2$•diglyme•H_2O. A careful optimization of the parameters, such as annealing temperature, aging time, and substrate nature, has been carried out in order to obtain, reproducibly and selectively, the $CsCaF_3$ pure phase as compact films. Structural, morphological and compositional characterizations of the thin films have been addressed through X-ray diffraction (XRD), field-emission scanning electron microscopy (FE-SEM) and Energy Dispersive X-ray (EDX) analysis. In particular, the high impact of the present work can be ascribed to the possibility of producing $CsCaF_3$ in form of thin film on large surfaces under quite mild condition of pressure and temperature. These aspects can open the route to the application of these materials in optoelectronic field. To the best of our knowledge, the present approach represents the first report on the sol–gel synthesis of $CsCaF_3$ in form of thin films. The application of β-diketonate fluorinated precursors provided a breakthrough for the solution route approach, allowing the fine control of the stoichiometry of the final perovskite systems. Furthermore, the applied fluorinated adducts act also as a fluorine source, thus avoiding the use of additional halogen source.

2 Materials and methods

2.1 Synthetic methodology

The sol–gel reaction occurred in the ethanol/water solution of Cs(hfa) and $Ca(hfa)_2$•diglyme•H_2O. The cesium and calcium complexes were prepared starting respectively from cesium hydroxide and calcium oxide, and the ligands Hhfa and diglyme in dichloromethane under reflux for 1 h. The detailed procedures are reported in Ref. [21, 22].

For the sol hydrolysis, the following molar ratio of precursors, solvent and catalyst was used:

x Cs(hfa): x $Ca(hfa)_2$•diglyme•H_2O: 43 C_2H_5OH: 1.5H_2O: 0.8 CF_3COOH.

Two different molar ratios of the precursors were tested: x = 0.5 mmol and 1 mmol in order to study the effect of the precursor concentration on the sol hydrolysis and thus on the composition and the homogeneity of the films. The sol was stirred at 60 °C for different aging times, i.e. 8 h and 20 h, and successively spin-coated on 1 cm × 1 cm Si (100) and glass substrates. The spin-coating process was carried out in two steps of deposition using a Spin-Coater SPIN-150 SPS Europe, at 3000 rounds per minute (RPM), with a speed rate of 1000 RPM/sec. For each step, 0.2 ml of the gel were spun for a time of 60 s on the substrate and after each step, the sample was heated in air for 10 min. A final annealing treatment has been performed for 1 h in air. The intermediate heating treatment and the final annealing were carried out in the temperature range of 350–550 °C. The temperature during all the heating treatment has been monitored using K-type thermocouples with ± 2 °C accuracy and a computer-controlled hardware.

2.2 Characterization

Structural characterization was carried out using a Smartlab Rigaku diffractometer in gracing incident mode (0.5°) equipped with a rotating anode of Cu Kα radiation operating at 45 kV and 200 mA. The patterns were recorded in the range from 15° to 60° with 0.05° step resolution. Film morphologies were investigated by field-emission scanning electron microscopy (FE-SEM) using a ZEISS SUPRA 55 VP microscope. The films deposited on glass were Au-coated before FE-SEM characterizations. For all the samples several regions were analyzed, confirming the homogeneity of the morphologies here reported. The atomic composition of the samples was performed through energy dispersive X-Ray (EDX) analysis using an electron beam acceleration of 15 keV. The EDX spectra were recorded using an INCA-Oxford windowless detector, having a resolution of 127 eV as the full width at half maximum (FWHM) of the Mn Kα. A CaF_2 single crystal was used as a standard for fluorine quantification. The EDX analysis was recorded at least on three different points for each sample in order to assess the quantitative compositions.

3 Results

3.1 Optimization of the sol–gel process for the formation of $CsCaF_3$ phase films

The present section displays in detail the most significant experimental data for the novel sol–gel/spin-coating approach adopted for the fabrication of pure $CsCaF_3$ phase in form of thin films. The starting point of the procedure is the use of a β-diketonate complex mixture of cesium and calcium, i.e. Cs(hfa) and $Ca(hfa)_2$•diglyme•H_2O, whose structures are reported in Fig. 1.

Here, an overview of the various routes applied to optimize the formation of the $CsCaF_3$ phase is summarized in Scheme 1. We show only the main representative routes tested in the present work, explaining in details the key parameters of each route for the production of pure $CsCaF_3$ thin films. In particular, the key parameters are the molar ratio of the starting solution, the aging time of the hydrolysis process, the nature of the substrates and the annealing temperature.

The first procedure (route 1 in scheme 1) with a Cs(hfa): $Ca(hfa)_2$•diglyme•H_2O molar ratio of 1: 1 (1 Cs(hfa): 1 $Ca(hfa)_2$•diglyme•H_2O: 43 C_2H_5OH: 1.5 H_2O: 0.8 CF_3COOH), aging time of 20 h and annealing temperature of 400 °C using Si (100) as substrate, results in the formation of a compact film containing different phases. In fact, the pattern in Fig. 2a displays several peaks attributed to the formation of three phases, i.e. CaF_2, Cs_2SiF_6 and $CsCaF_3$ polycrystalline structures, as confirmed by the match with the ICDD n. 35–0816, n. 07–0006 and n. 21–0817 for the CaF_2, Cs_2SiF_6 and $CsCaF_3$ phases, respectively. The peak values of the various phases observed in the pattern are compared to the CaF_2, Cs_2SiF_6 and $CsCaF_3$ bulk ones in table S1 reported in the supporting information. The related FE-SEM image (Fig. 3a) shows the formation of a homogeneous and compact layer on silicon substrate with a very porous structure and a thickness of about 950 nm. This aspect points to the fact that even if the film presents a mixture of crystalline phases the morphology appears uniform over a large area. The coexistence of CaF_2, Cs_2SiF_6 and $CsCaF_3$ phases has been also confirmed by EDX analysis (Fig. S1). In fact, the quantitative EDX analyses, carried out on different sites of the film surface, show a stoichiometry of Cs: Ca ranging from 1:1 on some sites up to 1:4 in others, suggesting the presence of a CaF_2 excess.

Successively, the effect of the aging time on the precursor hydrolysis process has been studied in order to analyse the effect on both the $CsCaF_3$ phase stabilization and morphology of the material. Therefore, a new sol–gel procedure (route 2) has been tested, in which the hydrolysis time has been reduced to 8 h with respect to the previous one, while the annealing temperature has been maintained at 400 °C, as reported in detail in Scheme 1. In this case, the XRD pattern of the related film (Fig. 2b) still shows the presence of CaF_2 and Cs_2SiF_6 phases together with the phase of interest, $CsCaF_3$.

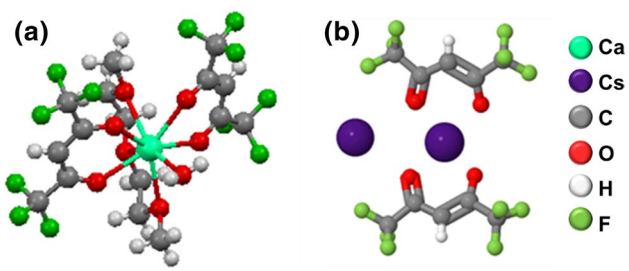

Fig. 1 Molecular structures of **a** $Ca(hfa)_2$•diglyme•H_2O and **b** Cs(hfa) precursors derived from ref. [21, 22] using the Mercury code [23]

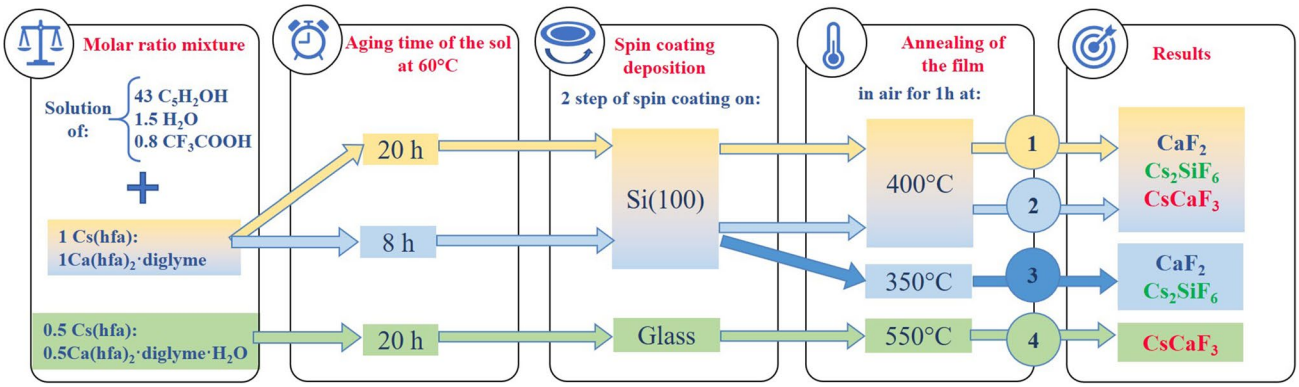

Scheme 1 Scheme of the sol–gel/spin-coating process of $CsCaF_3$ (routes from 1 to 4) at different molar ratios, aging time, substrates and annealing temperature

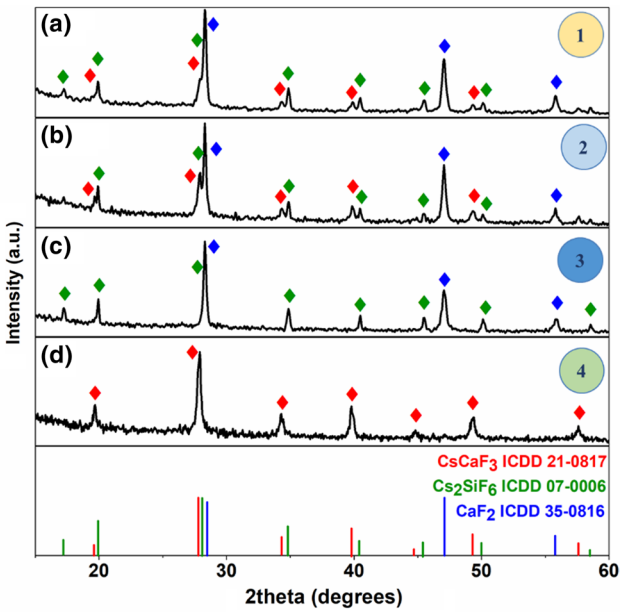

Fig. 2 XRD patterns of Cs-Ca films grown under different conditions: **a** route 1 with a molar ratio of the starting mixture 1: 1: 43: 1.5: 0.8, aging time 20 h, annealing temperature 400 °C, on Si (100) substrate; **b** route 2 with a molar ratio of 1: 1: 43: 1.5: 0.8, 8 h, 400 °C, on Si (100); **c** route 3 with a molar ratio of 1: 1: 43: 1.5: 0.8, 8 h, 350 °C, on Si (100); **d** route 4 with molar ratio 1: 1: 43: 1.5: 0.8, 20 h, 550 °C, on glass

On the other side, also in this case the FE-SEM image in Fig. 3b shows a smoother and flat surface of the film, while the EDX analysis presents an inhomogeneous distribution of Cs and Ca amounts on the whole surface (see Fig. S2). The cross-section image in Fig. 3b confirms the homogeneity of the layer with a thickness of about 900 nm. Thus, the difference in the morphology and EDX composition for the samples of routes 1 and 2 (Fig. 3a and b) can be ascribed to the difference in the aging time of the process. In fact, the reduction of the aging time diminishes the hydrolysis process between the precursors, resulting in a smoother and flat surface and inhomogeneity distribution of Cs and Ca.

The effect of the annealing temperature has been tested in the procedure described in Scheme 1 route 3 with the aim of analysing the effect of the heating treatment on the interaction between the film and Si substrate, and of stabilizing the $CsCaF_3$ phase. In this new procedure the annealing temperature has been reduced to 350 °C and the other operative parameters have been maintained unchanged. The XRD analysis associated with the route 3 is reported in Fig. 2c in which the pattern displays the presence of peaks related to the CaF_2 phase together with peaks attributed to the Cs_2SiF_6 phase. No signals related to the presence of $CsCaF_3$ are detected, thus indicating that 350 °C is a temperature too low for the formation of the $CsCaF_3$ perovskite phase. The related morphology, reported in Fig. 3c, displays the formation of a compact and homogenous surface. Furthermore, due to a coalescence phenomenon, barely visible rounded grains of about 50 nm are detected; the thickness is assessed at about 1000 nm. EDX analysis presents a not stoichiometric composition of Cs:Ca molar ratio, ranging from 1:0.6 to 1:0.45 on different sites of the surface (see Fig. S3). This behaviour

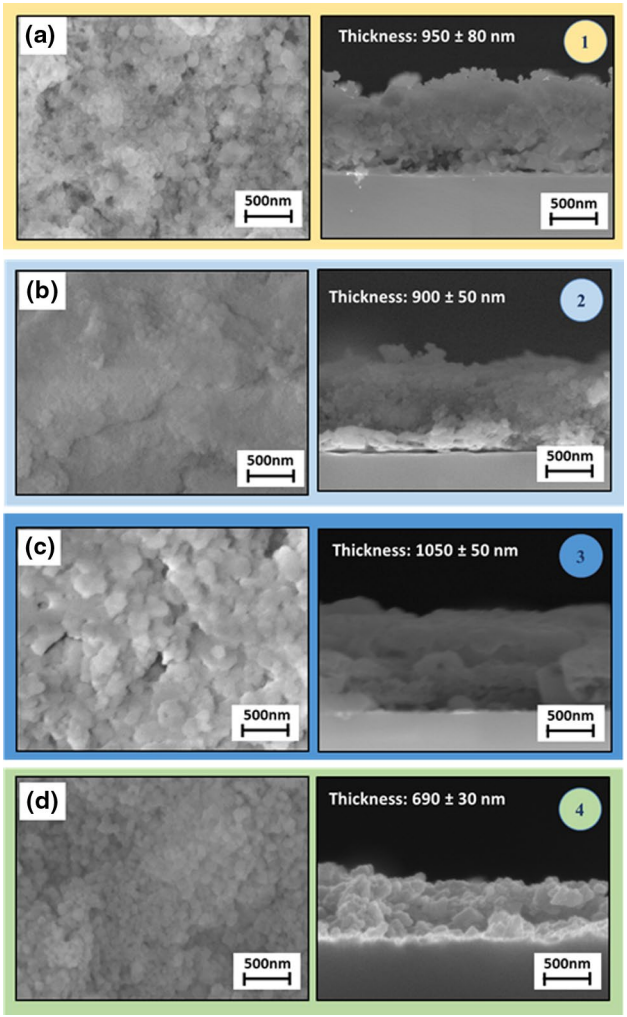

Fig. 3 FE-SEM plan and cross-sectional images of Cs-Ca films grown under different conditions: **a** route 1 with a molar ratio of the starting mixture 1: 1: 43: 1.5: 0.8, aging time 20 h, annealing temperature 400 °C, on Si (100) substrate; **b** route 2 with a molar ratio of 1: 1: 43: 1.5: 0.8, 8 h, 400 °C, on Si (100); **c** route 3 with a molar ratio of 1: 1: 43: 1.5: 0.8, 8 h, 350 °C, on Si (100); **d** route 4 with a molar ratio of 1: 1: 43: 1.5: 0.8, 20 h, 550 °C on glass

could be explained by considering that at lower annealing temperature, i.e. 350 °C, only the CaF_2 and Cs_2SiF_6 phases are stabilized, while the formation of the perovskite $CsCaF_3$ phase requires a higher thermal budget.

Based on this evidence, a new procedure has been set up (scheme 1, route 4) using: (i) a smaller amount of Cs and Ca precursors; (ii) a glass substrate with the aim of reducing the interaction with the Si substrate; (iii) an aging time up to 20 h; and (iv) an increase of the annealing temperature at 550 °C in order to avoid the formation of CaF_2 and promote the stabilization of the $CsCaF_3$ phase. The XRD analysis in Fig. 2d displays a pattern with an excellent match with the $CsCaF_3$ phase, thus pointing to the formation of highly crystalline $CsCaF_3$ phase. Additionally, a comparison can be done between the XRD pattern of this film vs. the XRD pattern of the films deposited through route 3. In particular, by comparing the pure $CsCaF_3$ phase obtained through the route 4 with the film obtained through the route 3 (Fig. S4), it is clear the attribution of the different phases and that route 4 produces a pure $CsCaF_3$ film without any impurity of CaF_2 and Cs_2SiF_6 phases. The FE-SEM image in Fig. 3d shows the formation of a homogenous layer with a nano-porous structure on the whole glass substrate. The cross section (Fig. 3d) of the pure $CsCaF_3$ film deposited on glass at 550 °C allows the thickness estimation of about 690 ± 30 nm and corroborates the formation of a compact deposit on the substrate surface.

Moreover, the EDX quantitative analysis (Fig. 4) confirms the correct stoichiometry of the Cs: Ca: F with a value of 1.0:1.0:3.1 coincident with a molar ratio of 1:1:3, compatible with the formation of $CsCaF_3$ on the whole film surface. The Kα signals of oxygen, silicon and sodium at 0.53, 1.04 and 1.73 keV respectively, derive from the glass substrate; the peak of the gold component is due to the sputtering treatment of the film surface carried out before the FE-SEM measurements.

Finally, the absence of a peak at 0.27 keV, associable with the carbon Kα, excludes the presence of any contamination that could arise from the Cs(hfa) and $Ca(hfa)_2$•diglyme•H_2O complexes, pointing to a clean decomposition process of the precursors during the sol–gel procedure.

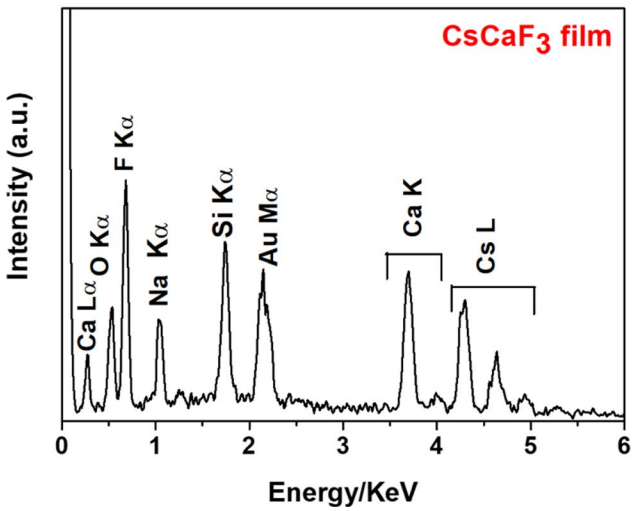

EDX quantitative analysis	
Element	**Atomic %**
O (K)	21.47
F (K)	**34.87**
Na (K)	9.32
Si (K)	8.73
Ca (K)	**11.44**
Cs (L)	**11.17**
Au (M)	3.10

Fig. 4 EDX spectrum of the $CsCaF_3$ film grown on glass substrate with a molar ratio of the starting mixture of 1: 1: 43: 1.5: 0.8, aging time 20 h, annealing temperature 550 °C (route 4)

4 Discussion

In the present work, the attention has been devoted to the optimization of the operative parameters of a novel sol–gel process for the fabrication of $CsCaF_3$ thin films using a β-diketonate complex mixture of Cs(hfa) and $Ca(hfa)_2$•diglyme•H_2O as precursors. Both the adducts are stable, white and not hygroscopic crystals. The main advantages of their use are related to their high solubility in the most common organic solvents, such as ethanol, and their reactivity under the hydrolysis process. In addition, their fluorine-rich structures avoid the use of an external fluorine source for the fabrication of $CsCaF_3$ perovskite. In this context, similarly, the $Ca(hfa)_2$•diglyme•H_2O has been successfully applied for the sol–gel synthesis of pure CaF_2 thin films [24, 25] and the Cs(hfa) has been used in combination with the $[Pb(hfa)_2diglyme]_2$ complex [26] for the fabrication of $CsPbBr_3$ microcrystals [27].

Herein, the most representative trials for the production of $CsCaF_3$ thin films have been reported and discussed in details. As described in the results of the first procedure, the initial operative conditions allowed the production of a homogeneous and porous composite made of a mixture of the three CaF_2, Cs_2SiF_6 and $CsCaF_3$ phases. The coexistence of the various phases can be also correlated to the EDX investigation, showing the presence of calcium-rich region. This result can be rationalized considering the presence in the same deposit of areas rich in the CaF_2 component. Afterwards, in the route 2 the effect of the aging time on the precursor hydrolysis process has been studied as a function of both the $CsCaF_3$ stabilization and the morphology of the film. However, the reduction of aging time if, on one side, has a strong effect on the morphology of the film with a smoother surface, on the other, does not help the stabilization of the $CsCaF_3$ structure. Furthermore, the presence of the Cs_2SiF_6 in the films obtained through routes 1 and 2 can be likely associated with an interaction between the silicon substrate and the material during the annealing treatment. Based on this evidence, a new procedure has been designed with the aim of decreasing the annealing temperature and thus reducing the interaction of the film with the substrate. Thus, the effect of a lower annealing temperature has been tested in the procedure 3 with the aim of analysing the effect of the temperature treatment on the interaction between the film and Si substrate, and of stabilizing the $CsCaF_3$ phase. Unfortunately, temperature reduction does not avoid the interaction of the film with the substrate, but it negatively affects the formation of the $CsCaF_3$ phase. This result can be explained by considering that at lower annealing temperature, only the CaF_2 and Cs_2SiF_6 phases are stabilized at the expense of the $CsCaF_3$ phase formation. In fact, the formation of CaF_2 through a sol–gel process has already been reported at temperature as low as 350 °C in our previous work in ref. 25. The observed findings indicate that the formation of the $CsCaF_3$ structure requires, instead, higher annealing temperature. In fact, the last optimized route 4, conducted with a higher annealing temperature of 550 °C together with the use of a glass substrate to avoid the interaction with the Si substrate, has resulted in the formation of pure $CsCaF_3$ thin films. In addition, also the *a*-axis parameter of the synthesized cubic $CsCaF_3$ phase has been evaluated and it is equal to 4.522 Å, in good accordance with the bulk value of 4.5244 Å (ICDD n. 21–0817). The formation of the pure phase has also been corroborated by EDX analysis. Furthermore, the use of the different substrates seems to affect the thickness of the final $CsCaF_3$ film on glass substrate. In fact, the $CsCaF_3$ system obtained through route 4 displays a thinner film, i.e. 690 nm vs the about 1000 nm of the other films. This trend can be

likely due to the different interaction between the gel and the substrate during the deposition process. In addition, also the smaller amount of Cs and Ca precursors used in route 4, and thus the lower density of the final gel, can affect the final thickness of the $CsCaF_3$.

5 Conclusions

In summary, this study represents the first ever synthetic process of deposition of perovskite pure-phase $CsCaF_3$ thin films through a novel optimized sol–gel/spin-coating approach with a high control of the process and film uniformity both in composition and morphology. The impact of the present work can be also ascribed to the innovative procedure which occurs under quite mild conditions of pressure and temperature. To the best of our knowledge, no other examples are reported in the literature on the synthesis of $CsCaF_3$ perovskite in form of thin films. The fluorinated β-diketonate compounds, Cs(hfa) and $Ca(hfa)_2$•diglyme•H_2O, have been used as starting point of the acid-catalyzed process, acting as sources of all the required ions, namely cesium, calcium and fluorine. Notably, the application of such β-diketonate fluorinated adducts provides a breakthrough for the solution route, allowing a fine control of the stoichiometry of the final system. A comprehensive study of the most representative experimental set-up has been described, paying attention to the effects of experimental parameters, such as annealing temperature, aging time and substrate nature, on the composition of the final fluoride material.

The advantages of the present approach are mainly related to the reliability, reproducibility and the possibility to easily modify the crystallinity and the morphology of the final films through a fine tuning of the key parameters. Furthermore, the herein described process presents an added value due to the potential scaling up for larger deposition surface using a spray coating process as alternative to the spin-coating approach. Finally, the importance of the present work can be related to the high tunability of the solution process, which can be extended ideally to other analogous halide perovskite systems just playing with both nature of fluorinated β-diketonate compounds and parameters of the process.

Acknowledgements The authors thank the University of Catania for financial support within the PIACERI research program UNICT 2020-22 Linea 2. A. L. P. thanks the Ministero dell'Università e della Ricerca within the PON FSE REACT-EU 2014-2020 Azioni IV-4. The authors thank Bionanotech Research and Innovation Tower (BRIT) laboratory of University of Catania (Grant no. PONa3_00136 financed by the Italian Ministry for Education, University and Research, MIUR) for the diffractometer facility.

Author contributions Conceptualization: ALP; investigation: ALP and FLP; writing—original draft preparation: ALP; writing—review and editing: GM; funding acquisition: GM. All authors have read and approved the final manuscript.

Data availability All data generated or analyzed during this study are included in this published article and its Additional files.

Declarations

Competing interests The authors declare no competing interests.

References

1. Liu Y, Trimby P, Collins L, Ahmadi M, Winkelmann A, Proksch R, Ovchinnikova OS. Correlating crystallographic orientation and ferroic properties of twin domains in metal halide perovskites. ACS Nano. 2021;15:7139.
2. Yin W, Yang J, Kang J, Yan Y, Wei S. Halide perovskite materials for solar cells: a theoretical review. J Mater Chem A. 2015;3:8926.
3. Shahrokhi S, Gao W, Wang Y, Anandan PR, Rahaman MZ, Singh S, Wang D, Cazorla C, Yuan G, Liu JM, Wu T. Emergence of ferroelectricity in halide perovskites. Small Methods. 2020;4:2000149.
4. Park H, Ha C, Lee J-H. J Mater Chem A. 2020;8:24353.
5. Xu Y, Cao M, Huang S. Recent advances and perspective on the synthesis and photocatalytic application of metal halide perovskite nanocrystals. Nano Res. 2021. https://doi.org/10.1007/s12274-021-3362-7.

6. Li X, Yu D, Cao F, Gu Y, Wei Y, Wu Y, Song J, Zeng H. Healing all-inorganic perovskite films via recyclable dissolution-recrystallization for compact and smooth carrier channels of optoelectronic devices with high stability. Adv Funct Mater. 2016;26:5903.
7. Salmankurt B, Duman S. Investigation of the structural, mechanical, dynamical and thermal properties of $CsCaF_3$ and $CsCdF_3$. Mater Res Express. 2016;3: 045903.
8. Han X, Song E, Zhou Y, Hu T, Xia Z, Zhang Q. Photon upconversion afterglow material toward visualized information coding/decoding. J Mater Chem C. 2020;8:3678.
9. Raja A, Nagaraj R, Ramachandran K, Sivasubramani V, Annadurai G, Joseph Daniel D, Ramasamy P. A novel bifunctional Dy^{3+} activated $RbCaF_3$ single phase phosphor: facile synthesis and dual-luminescence properties for WLEDs and dosimetry applications. Adv Powder Technol. 2020;31:2597.
10. Ridou C, Rousseau M, Bouillot J, Vettier C. Anharmonicity in fluoperovskites. J Phys C Solid State Phys. 1984;17:1001.
11. Li L, Wang YJ, Liu DX, Ma CG, Brik MG, Suchocki A, Piasecki M, Reshak AH. Comparative first-principles calculations of the electronic, optical, elastic and thermodynamic properties of $XCaF_3$ (X=K, Rb, Cs) cubic perovskites. Mater Chem Phys. 2017;188:39.
12. Arora G, Sharma M. Study of $KCaF_3$ and $CsCaF_3$ using hybrids density functionals. Mater Today. 2020;29:267.
13. Moschou G, Koliogiorgos A, Galanakis I. Electronic properties of Cs-based halide perovskites: an ab initio study. Phys Status Solidi A. 2018;215:1700941.
14. Körbel S, Marques MAL, Botti S. Stability and electronic properties of new inorganic perovskites from high-throughput ab initio calculations. J Mater Chem C. 2016;4:3157.
15. Ma CG, Brik MG. Hybrid density-functional calculations of structural, elastic and electronic properties for a series of cubic perovskites $CsMF_3$ (M = Ca, Cd, Hg, and Pb). Comput Mater Sci. 2012;58:101.
16. Murtaza G, Ahmad I, Afaq A. Shift of indirect to direct bandgap in going from K to Cs in $MCaF_3$ (M: K, Rb, Cs). Solid State Sci. 2013;16:152.
17. Park HH, Senegas J, Reau JM, Pezat M, Darriet B, Hagenmuller P. The $CsCaF_{3-x}H_x$ solid solution ($0 \le x \le 1.70$): structural characteristics and hydrogen diffusion investigation. Mat Res Bull. 1988;23:1127.
18. Falin ML, Gerasimov KI, Latypov VA. Determination of the position of the impurity Yb^{3+} ion in the $CsCaF_3$ crystals. Appl Magn Reson. 2014;45:707.
19. Catalano MR, Pellegrino AL, Rossi P, Paoli P, Cortelletti P, Pedroni M, Speghini A, Malandrino G. Upconverting Er^{3+}, Y^{b3}+ activated β-NaYF4 thin films: a solution route using a novel sodium β-diketonate polyether adduct. New J Chem. 2017;4:4771.
20. Pellegrino AL, Catalano MR, Cortelletti P, Lucchini G, Speghini A, Malandrino G. Novel sol-gel fabrication of Yb^{3+}/Tm^{3+} co-doped β-$NaYF_4$ thin films and investigation of their upconversion properties. Photochem Photobiol Sci. 2018;17:1239.
21. Vikulova ES, Zherikova KV, Kuratieva NV, Morozova NB, Igumenov IK. Synthesis, structure, and thermal properties of fluorinated cesium β-diketonates. J Coord Chem. 2013;66:2235.
22. Kuzmina NP, Tsymbarenko DM, Korsakov IE, Starikova ZA, Lysenko KA, Boytsova OV, Mironov AV, Malkerova IP, Alikhanyan AS. Mixed ligand complexes of AEE hexafluoroacetylacetonates with diglyme: synthesis, crystal structure and thermal behavior. Polyhedron. 2008;27:2811.
23. Mercury 3.7, free program of the Cambridge Crystallographic Database, New Features for the Visualization and Investigation of Crystal Structures.
24. Pellegrino AL, Lucchini G, Speghini A, Malandrino G. Energy conversion systems: molecular architecture engineering of metal precursors and their applications to vapor phase and solution routes. J Mater Res. 2021;35:2950.
25. Pellegrino AL, La Manna S, Bartasyte A, Cortelletti P, Lucchini G, Speghini A, Malandrino G. Upconverting tri-doped calcium fluoride-based thin films: a comparison of the MOCVD and sol–gel preparation methods. J Mater Chem C. 2020;8:3865.
26. Malandrino G, Lo Nigro R, Rossi P, Dapporto P, Fragala IL. A volatile Pb(II) β-Diketonate diglyme complex as a promising precursor for MOCVD of lead oxide films. Inorg Chim Acta. 2004;357:3927.
27. Pellegrino AL, Malandrino G. Surfactant-free synthesis of full inorganic perovskite $CsPbBr_3$: evolution and phase stability of $CsPbBr_3$ vs. $CsPb_2Br_5$ and their photocatalytic properties. ACS Appl Energy Mater. 2021;4:9431.